

Deformation-Induced Large Ductility of Super Saturated Solid Solution Fe-Cu Alloy

Licai Fu*, Jun Yang, Qinling Bi, Weimin Liu

State Key Laboratory of Solid Lubrication, Lanzhou Institute of Chemical Physics, Chinese Academy of Sciences, Lanzhou, China.
Email: *licaifu@licp.cas.cn

Received September 25th, 2011; revised October 29th, 2011; accepted November 7th, 2011.

ABSTRACT

The mechanical properties of super saturated solid solution Fe₆₀Cu₄₀ alloy has been investigated using compression test. The results show that the grain precipitation and phase transformation occurs during compressive deformation resulting in large work-hardening ability, high strength and large ductility. Our results demonstrate that this novel architecture offers a design pathway towards a new generation of strong materials with large ductility.

Keywords: Fe-Cu Alloy, Super Solid Solution, Precipitation, Phase Transform, Ductility

1. Introduction

Strength and ductility are of the most important mechanical properties of structural materials. However, they are often difficult to obtain the high strong and large ductility simultaneously [1,2]. Generally, the low ductility of materials is attributed to the lack of work hardening caused by their inability to accumulate dislocations [3]. Therefore, the basic idea to improve the ductility of materials is to regain the work hardening (dislocation accumulation capability), which is often accompanied with sacrifice of strength. Classical methods for strengthening materials contain solid solution, dislocation, grain boundary and so on [4]. The solid solution strength metals are to alloy them with elements that are dissolved in the crystal lattice and form a solid solution. Such atoms elastically distort the crystal and can thus interact with the stress field of a dislocation and impede its movement, which results in high strength [5]. On the other hand, large numbers of reports indicated precipitate and phase transformation are also beneficial to improve the ductility during deformation of alloys. Kim showed that certain size of precipitate can improve the hardness and work hardening of the materials [6]. Their excellent mechanical properties result from the martensitic transformation of metastable retained austenite, induced by thermomechanical loading [7,8].

Dendrite composite immiscible Fe₆₀Cu₄₀ alloy has been prepared successfully by combustion synthesis technique (CS) [9]. By controlling the applied pressure, the different

super saturated solid solution Fe₆₀Cu₄₀ alloys have been obtained. Especially, there are not large composite segregation both in dendrite and matrix. In this paper, we examined the mechanical properties of this special alloy under compression test. The results show that the nano-scale precipitation and phase transformation occurs during compressive deformation resulting in large work-hardening ability and high strength. Our results demonstrate that this novel architecture offers a design pathway towards both strong and ductility materials.

2. Experimental

The Fe₆₀Cu₄₀ alloy has been prepared successfully by CS [9]. In this paper, the Fe₆₀Cu₄₀ alloys with different microstructure have been produced by CS under different applied pressure with 8, 6 and 4 MPa of argon gas, which indicated as FC₈, FC₆ and FC₄, respectively. Morphologies and compositions of the Fe₆₀Cu₄₀ alloys were examined using a JSM-5600LV scanning electron microscope (SEM) equipped with an energy dispersive X-ray spectroscope (EDS, Kevex, USA). Cylindrical compressive specimens with length of 4.5 mm and a diameter of 2.8 mm were cut using an electro-discharging machine, and both ends of the compressive specimens were polished to mirror surfaces, and coated with graphite before tests to reduce the interfacial friction. Quasi-static uniaxial compression test were performed at room temperature using a testing machine with a crosshead speed of $3.5 \times 10^{-3} \text{ s}^{-1}$. The before and after compression test samples were in-

vestigated with X-ray diffractometry (XRD, Philips X'pert) using $\text{CuK}\alpha$ radiation. The cross sections of fractured $\text{Fe}_{60}\text{Cu}_{40}$ alloys were also analyzed by the SEM.

3. Results

The typical compressive engineering stress-strain curves of the $\text{Fe}_{60}\text{Cu}_{40}$ alloys are compared in **Figure 1**. The yield strength σ_y , ultimate fracture strength σ_{\max} , fractural strain ε_f are also given in table inset of **Figure 1**. The yield strengths of the FC_8 , FC_6 , and FC_4 samples are 520 MPa, 900 MPa, and 790 MPa, respectively, which are higher than that of commercial crystalline Cu-Fe alloys [10]. The highest yield strength is obtained with applied pressure 6 MPa. As shown, the uniform elongation of the FC_8 and FC_4 are only 4% to 5%. In contrast, the uniform elongation of the FC_6 reaches about 20%. It is more than fourfold that of the nanostructured sample and above the critical ductility required for many structural applications. The ductility of the FC_6 enhances because of an improved work-hardening rate. The strong working hardening allows uniform deformation, and leads to a fast climbing curve in the compression test, which is different with most nanostructured metals and alloys that show plunging curves peaking very early in plastic deformation [1]. So, the strain to failure reaches 30% in the compression.

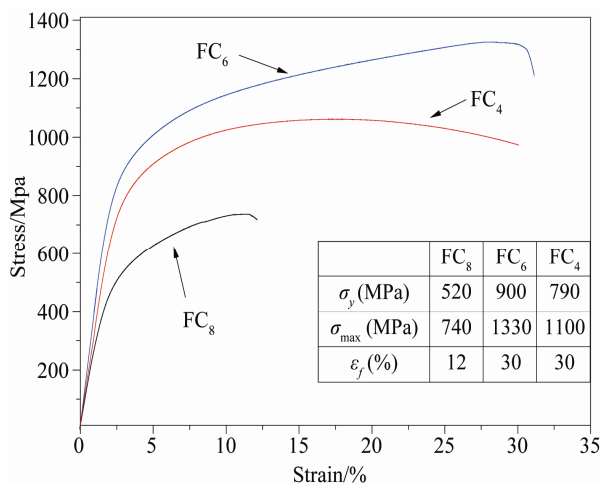


Figure 1. Compressive engineering stress-strain curves of the $\text{Fe}_{60}\text{Cu}_{40}$ alloy. Table of inset is the yield strength σ_y , ultimate fracture strength σ_{\max} , fractured strain ε_f of the $\text{Fe}_{60}\text{Cu}_{40}$ alloys.

Table 1. Composition of the $\text{Fe}_{60}\text{Cu}_{40}$ alloys.

	FC_8		FC_6		FC_4	
	dendrite	matrix	dendrite	matrix	dendrite	matrix
Cu	15.4	75.5	16.1	64.4	20.0	56.6
Fe	84.6	24.5	83.9	35.6	80.0	43.4

The SEM secondary electron images of the FC_8 and FC_6 and FC_4 are shown in **Figure 2**. All of the dendrites of the FeCu alloys are uniformly embedded into the matrix. It is maybe brought from the polishing because of the soft matrix (Cu solid solution). The matrix is composed of equiaxed ultrafine grains [9]. For FC_8 the primary dendrite axes have radii of about 2 - 5 μm , regular patterns of secondary dendrite arms with spacing 1 - 3 μm are observe, having radii of about 2 μm , which is smaller than the primary axis (**Figure 2(a)**). The primary and second dendrite axes become short and coarse as the applied pressure decreases (**Figure 2(b)**). The primary dendrite axes break and second dendrite axes get to rarely when the applied pressure decreases to the 4 MPa (**Figure 2(c)**). The composite of the dendrite and matrix are presented in **Table 1**. The results shows that the dendrite and matrix are Fe(Cu) solid solution and Cu(Fe) solid solution, respectively, for all the FeCu alloys. It should be noted that all the FeCu alloys are only, composed of elements Fe and Cu. It confirms the small black holes in the matrix are not impurity (**Figure 2**). The dendrite and matrix are Fe(Cu) solid solution (15.4 at% Cu) and Cu(Fe) solid solution (24.5 at% Fe), respectively, for the FC_8 . However, the solid solubility of the Fe(Cu) and Cu(Fe) increases to the 20 at% and 43.4 at%, respectively for the FC_4 . It means that both solid solubility of the Fe(Cu) and Cu(Fe) increase as the applied pressure decreases. Impressively, the solid solubility of the Cu(Fe) with applied 4 MPa is twice as with applied 8 MPa.

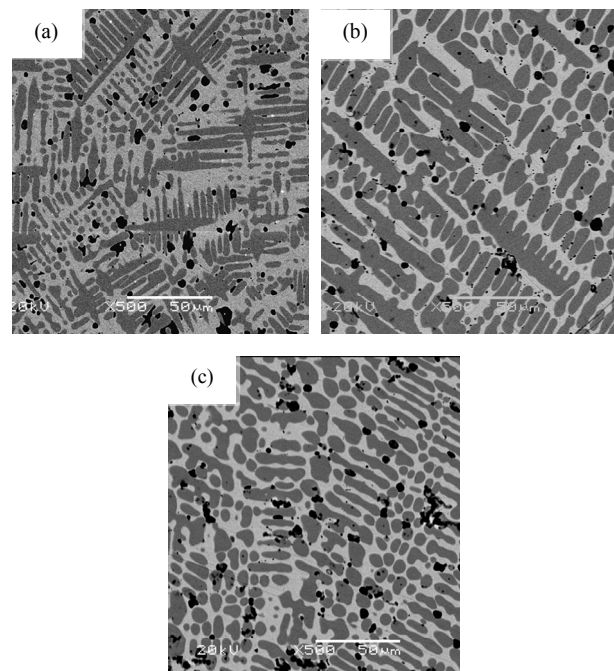


Figure 2. SEM images of the $\text{Fe}_{60}\text{Cu}_{40}$ alloys, (a) 8 MPa, (b) 6 MPa, (c) 4 MPa.

Figure 3 shows the XRD pattern of $\text{Fe}_{60}\text{Cu}_{40}$ alloys before and after compressive deformation. All the FC_8 , FC_6 , and FC_4 before and after compressive deformation contain the ε -Cu-rich and the α -Fe-rich phases. The diffraction peak γ -Fe-rich phase changes weak as the applied pressure decreases, and the γ -Fe-rich phase has not been examined using XRD when the applied pressure decreases to 4 MPa. However, the γ -Fe structure occurs after FC_4 deformation. Another impressively characterization is that the diffraction peaks of the ε -Cu-rich structure shift towards higher angles and γ -Fe-rich towards lower angle after $\text{Fe}_{60}\text{Cu}_{40}$ alloys deformation. It means that the solid solution of the ε -Cu-rich and γ -Fe-rich in $\text{Fe}_{60}\text{Cu}_{40}$ alloys decreases after the compressive deformation. It is to be noted that FC_6 has the highest ratio of ε -Cu-rich to γ -Fe-rich (defined as ratio of diffraction peaks).

The fractography of the $\text{Fe}_{60}\text{Cu}_{40}$ alloys is shown in **Figure 4**. The intergranular fracture feature has been observed in the fractured surface of the FC_6 (**Figure 4(a)**). The crack occurs along the dendrite axis because of the stress concentration in soft matrix in the compressive deformation. Some of the dendrite axis cracked when the stress concentration increases to the critical value, such as the zone of III. The **Figure 4(b)**, (c) and (d) are magnification of the I, II and III of the **Figure 4(a)**, respectively. Far from the fractured dendrite axis, large numbers of small grains precipitate from the dendrite and matrix (**Figure 4(b)**). Near the fractured dendrite axis (II), more precipitations occur, and lots of dimples has been observed with grain size of ultrafine scale comparing with the precipitation. The visible melt traces (**Figure 4(d)**) are regarded as matrix (melt pointing is about 1000°C) because the local temperature maybe is higher 1000°C the local stress concentration as the sample fractures. The

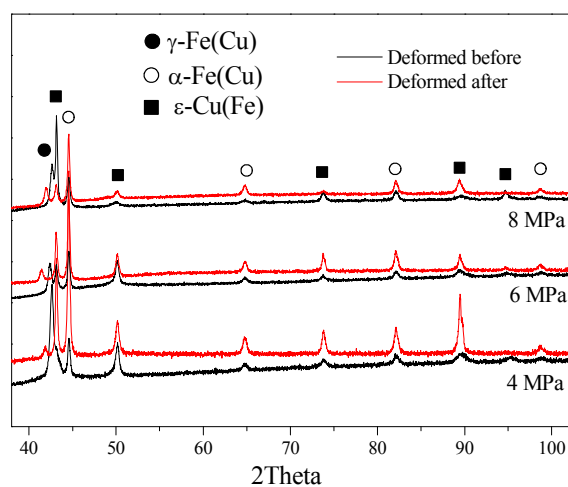


Figure 3. XRD patterns of the deformed before and after $\text{Fe}_{60}\text{Cu}_{40}$ alloys.

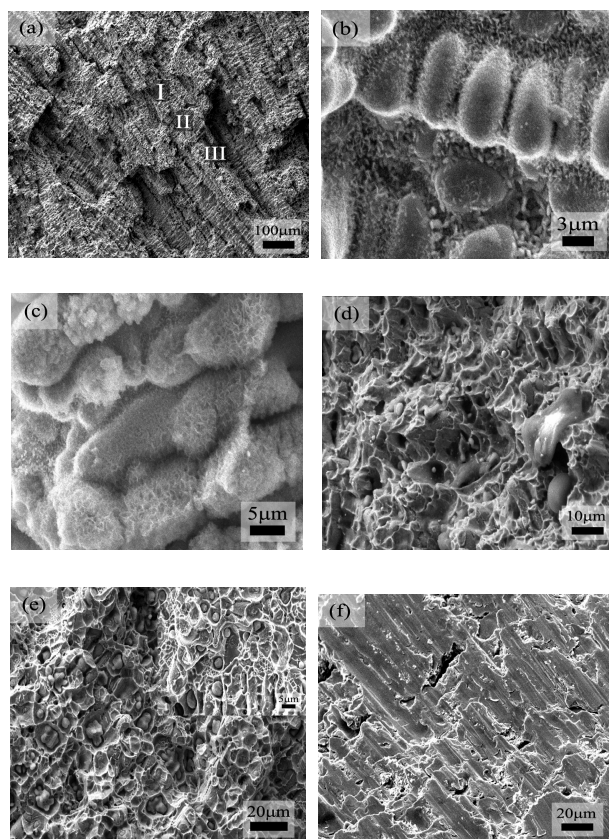


Figure 4. Fractography of the $\text{Fe}_{60}\text{Cu}_{40}$ alloys (a), (b), (c), (d) FC_6 ; (e) FC_4 ; (f) FC_8 .

dimples indicate good working harden of the FC_6 . The super saturated solid solution of the FC_4 with $\text{Cu}(\text{Fe})$ and $\text{Fe}(\text{Cu})$ is close to the FC_6 . Thus, the yield strength reaches 790 MPa, is near the yield strength of the FC_6 (900 MPa). However, the local stress concentration of the FC_4 is smaller than that of the FC_6 , because the dendrite axis of the FC_4 is coarse and short compared with the FC_6 . So, the working harden is decreases even the negative value. For the FC_8 , owing to the smaller dendrite axis and smaller solid solution, the strength and ductility are smaller than that of the FC_6 .

4. Conclusions

In this paper, the bulk immiscible $\text{Fe}_{60}\text{Cu}_{40}$ alloy is successfully prepared by a combustion synthesis technique. The $\text{Fe}_{60}\text{Cu}_{40}$ alloy is composed of Fe-rich dendritic embedded in Cu-rich matrix uniformly. The content of the dendrite and matrix are 34.5% and 65.5%, respectively. The grain size of matrix is about 30 nm. Owing to the very high superheating (4700°C) of combustion synthesis, the deeply undercooling is obtained, resulting there no large-scaled phase separation into Cu-rich and Fe-rich phases.

REFERENCES

- [1] M. A. Meyers, A. Mishra and D. J. Benson, "Mechanical Properties of Nanocrystalline Materials," *Progress in Materials Science*, Vol. 51, No. 4, 2006, pp. 427-556. [doi:10.1016/j.pmatsci.2005.08.003](https://doi.org/10.1016/j.pmatsci.2005.08.003)
- [2] C. C. Koch, I. A. Ovid'ko, S. Seal and S. Veprek, "Structural Nanocrystalline Materials: Fundamentals and Applications," Cambridge University Press, Cambridge, 2007. [doi:10.1017/CBO9780511618840](https://doi.org/10.1017/CBO9780511618840)
- [3] L. Capolungo, D. E. Spearot, M. Cherkaoui, D. L. McDowell, J. Qu and K. I. Jacob, "Dislocation Nucleation from Bicrystal Interfaces and Grain Boundary Ledges: Relationship to Nanocrystalline Deformation," *Journal of the Mechanics and Physics of Solids*, Vol. 55, No. 11, 2007, pp. 2300-2327. [doi:10.1016/j.jmps.2007.04.001](https://doi.org/10.1016/j.jmps.2007.04.001)
- [4] K. Lu, L. Lu and S. Suresh, "Strengthening Materials by Engineering Coherent Internal Boundaries at the Nanoscale," *Science*, Vol. 324, No. 5925, 2009, pp. 349-352.
- [5] J. Rösler, H. Harders and M. Bäker, "Mechanical Behaviour of Engineering Materials," Springer-Verlag, Berlin 2007.
- [6] J. Kim, M. Lee, D. Kim and R. Wagoner, "Micromechanics-Based Strain Hardening Model in Consideration of Dislocation-Precipitate Interactions," *Metals and Materials International*, Vol. 17, 2011, p. 291. [doi:10.1007/s12540-011-0417-4](https://doi.org/10.1007/s12540-011-0417-4)
- [7] Y. Ivanisenko, I. MacLaren, X. Sauvage, R. Z. Valiev and H. Fecht, "Shear-Induced $\alpha \rightarrow \gamma$ Transformation in Nanoscale Fe-C Composite," *Acta Materialia*, Vol. 54, No. 6, 2006, pp. 1659-1669. [doi:10.1016/j.actamat.2005.11.034](https://doi.org/10.1016/j.actamat.2005.11.034)
- [8] C. Yoo, Y. Park, Y. Jung and Y. Lee, "Effect of Grain Size on Transformation-Induced Plasticity in an Ultrafine-Grained Metastable Austenitic Steel," *Scripta Materialia*, Vol. 59, No. 1, 2008, pp. 71-74. [doi:10.1016/j.scriptamat.2008.02.024](https://doi.org/10.1016/j.scriptamat.2008.02.024)
- [9] L. Fu, J. Yang, Q. Bi and W. Liu, "Combustion Synthesis Immiscible Nanostructured Fe-Cu Alloy," *Journal of Alloys and Compounds*, Vol. 482, No. 1-2, 2009, pp. L22-L24. [doi:10.1016/j.jallcom.2009.04.016](https://doi.org/10.1016/j.jallcom.2009.04.016)
- [10] H. Kakisawa, K. Minagawa and K. Halada, "Tensile Behavior Change Depending on the Microstructure of a Fe-Cu Alloy Produced from Rapidly Solidified Powder," *Materials Science and Engineering: A*, Vol. 340, No. 1-2, 2003, pp. 175-180. [doi:10.1016/S0921-5093\(02\)00171-5](https://doi.org/10.1016/S0921-5093(02)00171-5)